JOURNAL OF CATALYSIS **169,** 157–165 (1997)
ARTICLE NO. CA971695

Hydrogen and Temperature Effects on the Coverages and Activities of Surface Intermediates during Methanation on Ru/SiO_2

Imre-Georges Bajusz and James G. Goodwin Jr.[1]

Department of Chemical and Petroleum Engineering, University of Pittsburgh, Pittsburgh, Pennsylvania 15261

Received October 29, 1996; revised February 24, 1997; accepted March 14, 1997

Methanation on Ru can be considered to be a representative example of many hydrogenation reactions. Steady-state isotopic transient kinetic analysis (SSITKA), one of the most powerful surface kinetic techniques capable of *in situ* assessing reaction parameters such as abundance of surface intermediates and intrinsic activity, was used to study the effects of hydrogen partial pressure and temperature on the fundamental surface reaction parameters for methanation (for a fixed P_{CO} of 0.036 bar) on Ru/SiO_2. Although absolute hydrogen coverage under reaction conditions is not able to be measured due to the hydrogen isotope effect, relative hydrogen surface concentration as a function of P_{H_2} was able to be estimated at constant temperature from SSITKA parameters. Increasing the hydrogen partial pressure at constant temperature caused an expected increase in the relative surface concentration of hydrogen and a concomitant increase in the abundance of CH_x species on the surface, N_M, possibly due to increased hydrogenation. At higher partial pressures of H_2, two active pools of methane intermediates (α and β) were able to be observed in the activity distribution analysis. However, at low P_{H_2}, only the most active species (α) was detected. It was found that N_M was additionally dependent on temperature and deactivation. At low H_2/CO ratios (H_2/CO = 5), no increase in N_M with increasing temperature was detected, which is suggested to be an effect of site blockage by the formation of greater amounts of inactive surface carbon at higher temperatures. At low temperatures, both α- and β-carbon were observed in the activity distribution analysis. However, at higher temperatures the less active β-carbon could not be detected. This can probably be explained by a transformation of β carbon into inactive γ carbon under these conditions. At high H_2/CO ratios (H_2/CO = 20), an increase in N_M was observed with increasing temperature. This was attributed mainly to a more efficient hydrogenation of the surface active carbon.

INTRODUCTION

Fundamental kinetic measurements under reaction conditions are very useful to describe accurately the surface phenomena occurring during a given heterogeneous catalytic process. For high surface area heterogeneous catalysts, a powerful technique, steady-state isotopic transient kinetic analysis (SSITKA), has emerged in the last two decades allowing *in-situ* measurements of the concentration and lifetime of surface intermediates while maintaining reaction at steady-state (1–4). SSITKA also permits a detailed examination of the surface site (intermediate) heterogeneity. If the catalyst sites are assumed to act independently in parallel and the reaction may be approximated by a pseudo-first-order process, the transient product rate response can be expressed by (5).

$$R^*(t) = N_P \int_0^\infty k e^{-kt} f(k) dk, \qquad [1]$$

where $R^*(t)$ is the transient of the rate of isotopically labeled product formation (μmol g^{-1} cat s^{-1}), N_P is the surface concentration of all the intermediates leading to product (μmol g^{-1}cat), k is the pseudo-first-order site activity (s^{-1}), and $f(k)$ the activity distribution. Numerical deconvolution techniques (6, 7) allow the determination of $f(k)$ from Eq. [1].

Methanation is a relatively simple yet important reaction for studying surface reaction phenomena. The activity of group VIIIA metals and support effects for methanation have been studied in detail by Vannice (8–10). Ru and Co show the highest activities. Ru is very appropriate for fundamental studies since it does not form oxide phases with supports as is often the case for Co (11).

The surface reaction mechanism of methanation was the subject of a lot of controversy until the 1980s when the following mechanism (proposed by a number of different authors such as those of references (12, 13)) gained wide acceptance:

$$\text{I.} \quad CO + * \leftrightarrows CO*$$

$$\text{II.} \quad CO* + * \leftrightarrows C* + O*$$

$$\text{III.} \quad H_2 + 2* \leftrightarrows 2H*$$

$$\text{IV.} \quad C* + H* \rightarrow CH* + *$$

$$\text{V.} \quad CH* + H* \rightarrow CH_2* + *$$

[1] To whom all correspondence should be addressed.

0021-9517/97 $25.00

VI. $CH_2* + H* \rightarrow CH_3* + *$

VII. $CH_3* + H* \rightarrow CH_4 + 2*$

VIII. $2H* + O* \leftrightarrows H_2O + 3*$

For Ru and Co catalysts hydrogenation of carbonaceous surface species has been widely concluded to be the rate-limiting step. Because of this, methanation can be considered to be representative of many hydrogenation reactions.

The hydrogenation of CO to form methane has been proven already to be an ideal system for isotopic transient kinetic investigations due to the simple molecules involved which are easy to trace by mass spectrometry (14–17). It was found with SSITKA that two types of carbon intermediate pools leading to methane exist on the surface: a more active pool α and a less active pool β (18–20). It is well known from the literature that adsorbed carbon can have different forms on a metal surface. For example, McCarty and Wise (21) prepared four types of carbon on an alumina-supported Ni catalyst: chemisorbed carbon, bulk Ni_3C, amorphous carbon, and graphitic carbon. However, the intrinsic difference in the nature of the two reactive pools α and β formed during methanation is still not clear.

It is of primary importance to understand the impact of hydrogen partial pressure and temperature on CO hydrogenation since both play key roles in this reaction as well as in many other hydrogenation processes. The objective of this study was to examine the effects of hydrogen partial pressure and temperature on the fundamental reaction parameters governing methanation on Ru/SiO_2. Emphasis was placed on determining their effects on the surface concentration of carbonaceous intermediates. The surface concentration of hydrogen under reaction conditions cannot be measured directly with SSITKA because of strong isotope effects during H_2/D_2 switches. However, by varying the hydrogen partial pressure, it was possible to estimate from SSITKA relative values for the hydrogen concentration on the surface under the various reaction conditions.

EXPERIMENTAL

Catalyst Preparation

The catalyst employed for this study was the same as used by Chen and Goodwin (22–24). It was prepared from $Ru(NO)NO_3$ (Alfa Chemical), dissolved in distilled water, and Cab-O-Sil HS5 fumed silica using the incipient wetness impregnation method. After impregnation, the catalyst precursor was dried at 363 K overnight. It was then prereduced in flowing hydrogen (50 cc/min) with a temperature ramp of 1 K/min to 673 K and kept for 8 h at this temperature. The catalyst was thoroughly washed with hot distilled water in order to remove any trace of Cl ions. It was then dried again at 363 K overnight.

Catalyst Characterization

Elemental analysis was done by Galbraith Laboratories, Inc. A Ru loading of 3 wt% was determined by atomic absorption. Using irreversible H_2 chemisorption at room temperature, the Ru dispersion was determined to be 36% (23). This corresponds to an average Ru particle size of 2.4 nm.

Reaction System

A schematic representation of the SSITKA system can be found in Ref. (24). The catalyst was placed in a quartz micro-reactor with ID of 4 mm. A thermocouple was installed on the top of the catalyst bed. A pneumatic valve operated electronically was used for the switch between feed streams containing different isotopic labeling of the reactant species (^{12}CO vs ^{13}CO). The pressure was maintained constant in the two streams to be switched by using two back pressure regulators. The on-line analytical part of the system consisted of a gas chromatograph (Varian 3700 GC) and a mass spectrometer (Leybold-Inficon Auditor 2 MS). In the GC the products were separated by a 6-foot, 60–80 mesh Porapaq Q column and detected with a flame ionization detector (FID). The mass spectrometer was equipped with a high-speed data-acquisition system interfaced to a personal computer. The holdup of the gases in the entire system was minimized. The lines of the outlet streams were heated to 150°C in order to avoid the possibility of heavy product deposition and blockage of the tubing. All the gases used for this study were of ultra high purity grade. They were further purified with traps. Before entering the reaction system, H_2 and CO were further purified using an Alltech Gas Purifier packed with indicating Drierite and 5A molecular sieve and a Matheson 450 Purifier filled with 4A molecular sieve, respectively.

Kinetic Measurements

Rate measurements of methanation were made using 25 to 35 mg of the catalyst loaded into the micro flowreactor. Before each experiment the catalyst was rereduced *in situ* with the same procedure employed for the initial reduction described above. After rereduction the catalyst bed temperature was lowered to the desired reaction temperature and the feed was switched to the reaction mixture. The total flow rate was kept at 100 cc/min for all the experiments. The feed consisted of 2 cc/min CO and, respectively, 8, 10, 14, 20, 25, and 40 cc/min H_2 with the balance being helium. The total pressure was maintained at 1.8 bar (1 bar $= 10^5$ Pa).

Steady-state reaction and isotopic transient data were collected at 240, 250, 260, and 270°C after 5 min of reaction in order to study the catalyst surface in its most pristine state. At these conditions the conversion was kept very low (less than 10%) and differential reactor behavior could be assumed. At this space velocity and the reaction conditions utilized, mass and heat transport limitations were

not detected. Specific activities were determined in terms of rate of CH_4 formation per gram of catalyst and TOF_H of CH_4 formation based on H_2 chemisorption. After each reaction period, the catalyst was bracketed with H_2 in order to minimize deactivation and to insure consistently a clean catalyst surface for the kinetic characterization at the different reaction temperatures. After each set of experiments, activity and SSITKA parameters were remeasured at the conditions of the first experiment to check for any irreversible deactivation of the catalyst. For the temperature dependence study, the kinetic measurements were taken with decreasing temperature. A time-on-stream study for two different temperatures and two hydrogen partial pressures was performed in order to observe the possible impact of reaction conditions on the deactivation process.

Steady-state isotopic transients were taken by switching between two feed streams where the only difference was the isotopic composition of CO: one stream containing ^{12}CO and the other ^{13}CO. A trace of argon (5%) was present in the ^{12}CO stream in order to measure the gas-phase holdup of the entire reaction system. This was not enough to disrupt the reaction during the isotopic switches.

The site heterogeneity was evaluated by deconvoluting Eq. [1] to obtain $f(k)$, the reactivity distribution function of the active sites. A standard Tikhonov regularization method (25) was used to build an objective functional in order to minimize the sum of square residuals and control the smoothness of $f(k)$. This procedure was necessary in order to avoid an ill-posed problem caused by an excess of random noise in the transient responses. Details about the algorithm can be found in Ref. (7).

RESULTS

Temperature Effects

Tables 1 and 2 give the results showing the impact of temperature on the measured reaction and SSITKA parameters after 5 min of reaction for two hydrogen partial pressures. The methane selectivity was greater than 90% at all reaction conditions. As expected the methanation rates and the TOF_H increased with increasing temperature. The apparent activation energies for these two hydrogen partial pressures were found to be 18.6 kcal/mol ($P_{H_2} = 0.18$ bar) and 19.5 kcal/mol ($P_{H_2} = 0.72$ bar), which correspond to typical values reported in the literature (9, 12). These values are within experimental error of each other.

In Tables 1 and 2, τ_{CO} and N_{CO} represent, respectively, the average surface residence time of CO and the number of CO molecules adsorbed on the surface at steady state. τ_M and N_M are the corresponding parameters for the carbon in all the surface intermediates leading to methane. Shannon and Goodwin (4) have described extensively the methodology used to calculate these parameters using SSITKA.

TABLE 1

Effect of Temperature on Specific Reaction Parameters for $H_2/CO = 5$ ($P_{H_2} = 0.18$ bar and $P_{CO} = 0.036$ bar)

Temperature (°C)	Methanation rate (μmol/(g cat. · s))[a]	TOF_H[b] (10^{-3} s^{-1})	τ_{CO} (s)[c]	N_{CO} (μmol/g cat.)[d]	τ_M (s)[c]	N_M (μmol/g cat.)[e]
240	0.6	5.5	4.8	237	7.4	4.4
250	0.9	8.3	4.4	217	5.6	5.0
260	1.2	11	4.6	227	3.2	3.8
270	1.7	16	4.1	202	2.8	4.8

Note. The errors given below correspond to standard deviations.
[a] ± 0.1 μmol/(g cat. · s).
[b] Based on irreversible H_2 chemisorption at 77 K (see Ref. (22)), $\pm 0.5 \times 10^{-3}$ s^{-1}.
[c] ± 0.1 s.
[d] ± 5 μmol/g cat.
[e] ± 0.6 μmol/g cat.

In terms of carbon monoxide, taking into account experimental error and significant data scatter, small apparent decreases in N_{CO} and τ_{CO} were observed with increasing temperature, as would be expected. Since τ_{CO} is the average surface residence time for all molecules of CO exiting the reactor, some of the variability in τ_{CO} is possibly due to changes with temperature in the fraction of the CO molecules in the gas stream which adsorb. This impacts the value of τ_{CO} since it is averaged over all CO molecules exiting the reactor, including those which did not adsorb during their passage through the catalyst bed. On the other hand, N_{CO} is very accurate within experimental error since its determination is based solely on a mass balance and requires no assumption in its interpretation.

At a hydrogen partial pressure of 0.18 bar (Table 1), the average surface residence time of the carbon in the

TABLE 2

Effect of Temperature on Specific Reaction Parameters for $H_2/CO = 20$ ($P_{H_2} = 0.72$ bar and $P_{CO} = 0.036$ bar)

Temperature (°C)	Methanation rate (μmol/(g cat. · s))[a]	TOF_H[b] (10^{-3} s^{-1})	τ_{CO} (s)[c]	N_{CO} (μmol/g cat.)[d]	τ_M (s)[c]	N_M (μmol/g cat.)[e]
240	1.4	13	3.7	202	3.8	5.3
250	2.3	21	4.1	189	3.6	8.3
260	3.6	33	4.2	194	3.1	11.2
270	5.3	49	3.9	180	2.6	13.8

Note. The errors given below correspond to standard deviations.
[a] ± 0.1 μmol/(g cat. · s).
[b] Based on irreversible H_2 chemisorption at 77 K (see Ref. (22)), $\pm 0.5 \times 10^{-3}$ s^{-1}.
[c] ± 0.1 s.
[d] ± 5 μmol/g cat.
[e] ± 0.6 μmol/g cat.

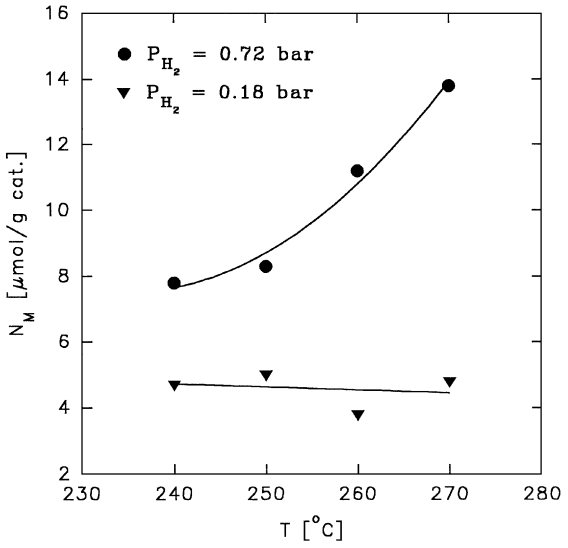

FIG. 1. Temperature dependency of the surface concentration of methane intermediates at different partial pressures of H_2.

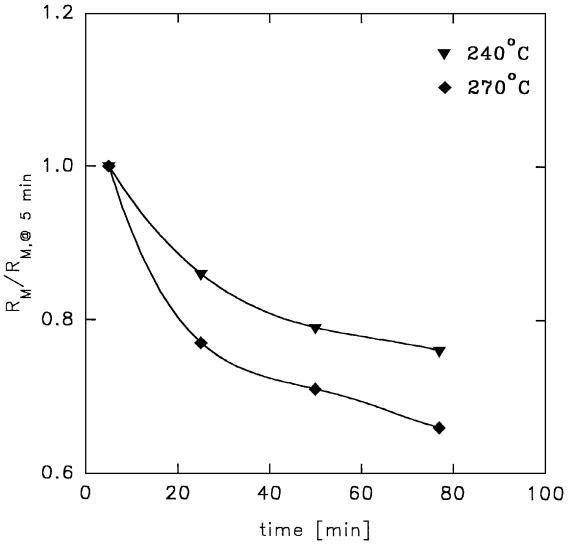

FIG. 2. Time-on-stream (TOS) behavior for different temperatures ($P_{H_2} = 0.18$ bar and $P_{CO} = 0.036$ bar, $H_2/CO = 5$).

intermediates leading to methane, τ_M, decreased monotonically with temperature, but the surface concentration of these carbon-containing intermediate species, N_M, remained fairly constant. At a hydrogen partial pressure of 0.72 bar (Table 2), a similar decrease in τ_M was observed. However, N_M exhibited a monotonic increase with temperature (Fig. 1).

If the hydrogenation of surface intermediates can be considered to be the rate-determining step (which appears to be the case under these conditions for Ru (26–28)), the overall rate for methane formation may be expressed by

$$R_M = k_M \cdot N_H \cdot N_M, \qquad [2]$$

where N_H is the surface concentration of hydrogen. Since

$$\tau_M = \frac{N_M}{R_M}, \qquad [3]$$

the relationship between the intrinsic rate constant k_M and τ_M is

$$\frac{1}{\tau_M} = k_M \cdot N_H = k. \qquad [4]$$

Thus, the inverse of the average surface residence time of the carbon-containing intermediates leading to methane represents a pseudo-first-order intrinsic activity, k, although it does include the hydrogen surface concentration dependence.

Figure 2 shows the time-on-stream behavior of the relative catalyst activity at the two extremes of the temperature range, 240 and 270°C, for the lowest H_2 partial pressure studied ($H_2/CO = 5$). A significant amount of deactivation was observed at 270°C, with relative decrease of 35%. At 240°C the deactivation was somewhat smaller with a relative decrease of 24%.

H_2 Partial Pressure Effects

Table 3 shows the reaction parameters for methanation at 240°C with a constant CO partial pressure of 0.036 bar but different hydrogen partial pressures. The order of reaction with respect to hydrogen was calculated to be around 0.9 for all the temperatures (Fig. 3). These values are in fairly good agreement with typical values in the literature (8, 12). The average surface residence time of the intermediates leading to methane consistently decreased with increasing hydrogen partial pressure. On the other hand, there was an apparent increase in the surface abundance of methane intermediates. For CO, the average surface

TABLE 3

Effect of P_{H_2} on Specific Reaction Parameters ($T = 240$°C and $P_{CO} = 0.036$ bar)

P_{H_2} (bar)	Methanation rate (μmol/(g cat. · s))[a]	TOF$_H$[b] (10^{-3} s^{-1})	τ_{CO} (s)[c]	N_{CO} (μmol/g cat.)[d]	τ_M (s)[c]	N_M (μmol/g cat.)[e]
0.14	0.4	3.7	3.6	196	8.8	3.5
0.18	0.5	4.6	3.8	207	7.4	3.7
0.25	0.6	5.5	3.6	196	6.1	3.8
0.35	0.8	7.4	3.6	196	5.0	4.0
0.45	1.0	9.2	3.9	212	4.3	4.3
0.72	1.4	13	3.7	202	3.8	5.3

Note. The errors given below correspond to standard deviations.
[a] ±0.1 μmol/(g cat. · s).
[b] Based on irreversible H_2 chemisorption at 77 K (see Ref. (22)), $\pm 0.5 \times 10^{-3}$ s^{-1}.
[c] ±0.1 s.
[d] ±5 μmol/g cat.
[e] ±0.6 μmol/g cat.

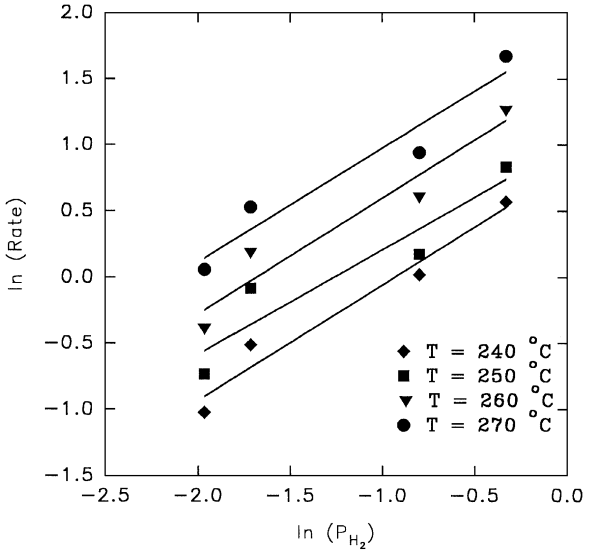

FIG. 3. Hydrogen partial pressure dependency of the methanation rate.

residence time and the surface concentration of reversibly adsorbed CO remained pretty much constant over the whole H_2 partial pressure range indicating little effect of H_2 partial pressure on CO adsorbing and desorbing without reaction.

Time-on-stream behavior was also studied for two hydrogen partial pressures: 0.18 and 0.45 bar (Fig. 4). The relative decrease in activity during TOS at 270°C was found to be 34% and 21% for 0.18 and 0.45 bar, respectively. Table 4 shows the impact of TOS on the SSITKA parameters for the hydrogen partial pressure of 0.45 bar. In terms of CO, no significant variation was observed. However, while the average surface residence time of the methane intermediates remained constant, their abundance decreased consistently during the first 50 min after the start of reaction.

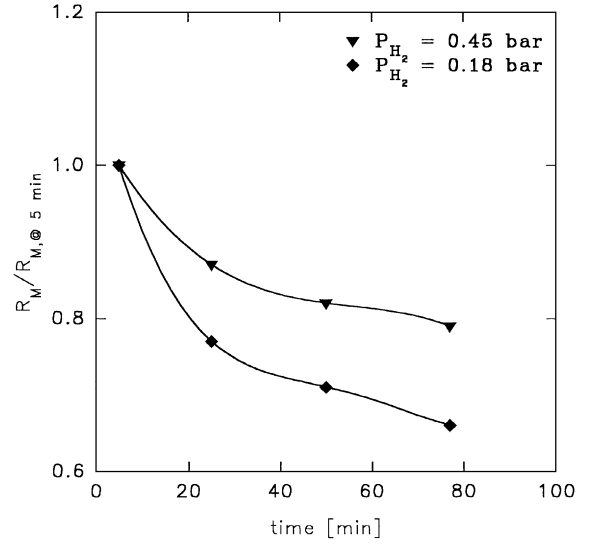

FIG. 4. Time-on-stream (TOS) behavior for different H_2 partial pressures ($P_{CO} = 0.036$ bar and $T = 270$°C).

TABLE 4

Effect of Time-on-Stream ($T = 270$°C, $P_{H_2} = 0.45$ bar and $P_{CO} = 0.036$ bar, $H_2/CO = 12$)

Time-on-stream (min)	Methanation rate (μmol/(g cat. · s))[a]	TOF_H[b] (10^{-3} s^{-1})	τ_{CO} (s)[c]	N_{CO} (μmol/g cat.)[d]	τ_M (s)[c]	N_M (μmol/g cat.)[e]
5	2.9	27	3.9	205	4.0	11.6
25	2.5	23	3.5	184	3.9	9.8
50	2.4	22	3.7	195	3.7	8.9
77	2.3	21	3.6	189	3.9	9.0

Note. The errors given below correspond to standard deviations.
[a] ± 0.1 μmol/(g cat. · s).
[b] Based on irreversible H_2 chemisorption at 77 K (see Ref. (22)), $\pm 0.5 \times 10^{-3}$ s^{-1}.
[c] ± 0.1 s.
[d] ± 5 μmol/g cat.
[e] ± 0.6 μmol/g cat.

DISCUSSION

Overall, a high selectivity to methane (>90%) was observed. This was mainly due to the high H_2/CO ratios (>3) used in the study. Higher hydrocarbon formation is more favored generally for lower H_2/CO ratios (29).

The activation energies based on methane production rate were almost identical (18.6 and 19.5 kcal/mol) for the two hydrogen partial pressures. This suggests that the mechanism and rate limiting step of methanation do not depend on the hydrogen concentration in the gas phase for the partial pressure range used in the study. This is also supported by the fact that the order of reaction with respect to H_2 remained constant at around 0.9 between 240 and 270°C (Fig. 3).

In terms of methane intermediates, the limitations related to τ discussed above for CO are less constraining. The impact of nonadsorbing molecules is absent since in order to be formed every methane molecule has to have been adsorbed. In addition, readsorption is not a major effect since methane essentially does not readsorb. As can be seen in Table 1, as the temperature increased at a relatively low H_2 partial pressure ($H_2/CO = 5$), τ_M decreased systematically while N_M remained constant. At higher H_2 partial pressure ($H_2/CO = 20$) (Table 2), in addition to the decrease in τ_M with increasing temperature, there was an increase in N_M (Fig. 1). N_M also increased systematically at 240°C when the hydrogen partial pressure was increased (Table 3).

The decrease in τ_M with an increase in H_2 partial pressure (Table 3) is directly related to its dependence on N_H. This

TABLE 5

Effect of P_{H_2} on the Relative Hydrogen Surface Concentration ($T = 240°C$ and $P_{CO} = 0.036$ bar)

P_{H_2}(bar)	$N_H/N_{H,0.18}$
0.14	0.84
0.18	1.00
0.25	1.21
0.35	1.48
0.45	1.72
0.72	1.95

offers an avenue for calculating relative hydrogen surface coverage. This quantity is able to be calculated from a ratio of τ_M's at a given temperature but two different hydrogen partial pressures based on Eq. [4] since k_M is only dependent on temperature:

$$\frac{(1/\tau_M)}{(1/\tau_M)_{\text{at ref. } P_{H_2}}} = \frac{(k_M \cdot N_H)}{(k_M \cdot N_H)_{\text{at ref. } P_{H_2}}} = \frac{N_H}{N_{H,\ P_{H_2},\ \text{ref.}}}; \quad [5]$$

$N_H/N_{H,0.18}$ is presented in Table 5, where $N_H/N_{H,0.18}$ represents the relative surface concentration of hydrogen on the catalyst referenced to a hydrogen partial pressure of 0.18 bar and a temperature of 240°C.

The observed increase of N_M with increasing hydrogen partial pressure at 240°C from Table 3 can now be compared with the monotonic increase of the relative surface hydrogen concentration as depicted in Fig. 5. It is worthwhile to reiterate that N_M represents the sum of all carbon-containing surface intermediates leading to methane, although the intermediates prior to the rate-determining step constitute the bulk of this quantity. It would appear that, with more hydrogen adsorbed on the surface, the surface carbon was able to be more efficiently hydrogenated, causing an increase in the concentration of active CH_x species. This is not inconsistent with the RDS being hydrogenation of CH_x species. Rather the presence of additional surface hydrogen probably decreases the amount of inactive surface carbon species formed which serves only to block portions of the surface.

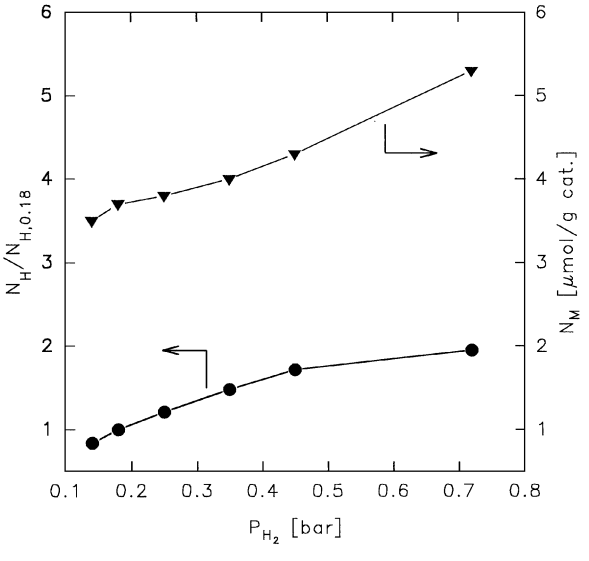

FIG. 5. N_M and $N_H/N_{H,0.18}$ dependency on the hydrogen partial pressure ($P_{CO} = 0.036$ bar and $T = 240°C$).

The impact of temperature on N_M was dependent on the hydrogen partial pressure and H_2/CO ratio (Fig. 1). With increasing temperature N_M increased for $P_{H_2} = 0.72$ bar ($H_2/CO = 20$), where it remained fairly constant for $P_{H_2} = 0.18$ bar ($H_2/CO = 5$). For $H_2/CO = 20$, the increase of N_M in temperature would appear to be related to the higher surface concentration of hydrogen which should promote the hydrogenation of surface carbon. It could be suggested that, at high temperatures, more sites were detectable due to the faster rates; however, this does not appear to be the case based on results given in Fig. 7 and discussed in the next paragraph. At $H_2/CO = 5$ any such potential increase appears to have been masked by a concomitant partial deactivation of the active sites with increasing temperature due to the low hydrogen partial pressure. This corresponds to our observation in the TOS study (Figs. 2 and 4), where a bigger relative decrease in activity with TOS was seen at low hydrogen partial pressure and high temperature. It has already been shown that the formation of inactive carbon on the catalyst surface is slowed enormously in the presence of hydrogen (30, 31).

The reaction scheme in Fig. 6 (previously proposed by Soong *et al.* (32)) is used to help illustrate the observations derived from the analysis of the activity distributions. The existence of three different carbon pools may be suggested upon CO dissociation. Methane is formed mainly from hydrogenation of α and β carbon (steps [1] and [2]). The less active β carbon is thought to be able to react to form γ carbon (step [3]) which does not hydrogenate to methane at a measurable rate. While a fine point, it cannot be excluded that α and β carbon may represent carbon bound

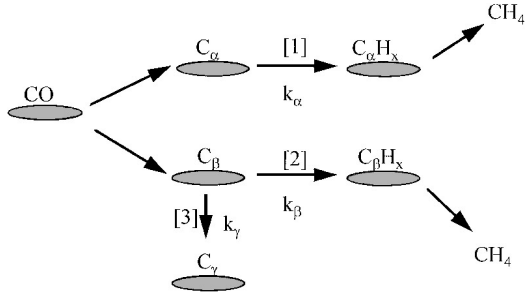

FIG. 6. Schematic representation of the two active pool model.

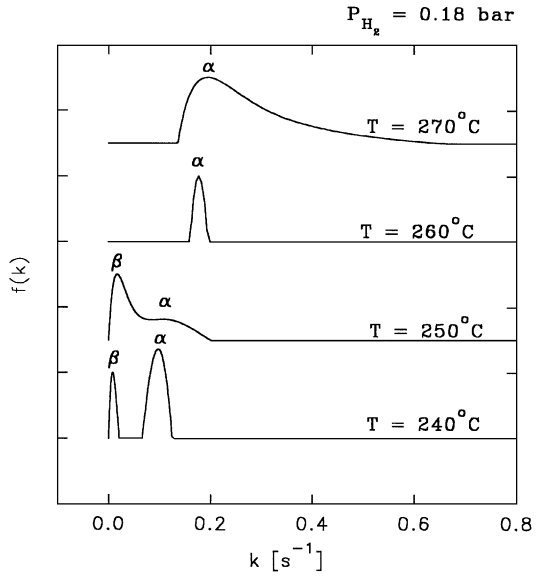

FIG. 7. Activity distributions for different temperatures ($P_{H_2} = 0.18$ bar, $P_{CO} = 0.036$ bar, $H_2/CO = 5$).

to sites having different activities and hydrogen capabilities. However, since CO hydrogenation is usually found to be structure insensitive (33), it is the usual convention to assume that CO may dissociate and form several kinds of carbon on perhaps similar sites. The activity distributions for methane formation ($f(k)$ in Eq. [1]) for the reaction conditions represented on Table 1 were evaluated numerically with the T-F deconvolution technique (7) and are displayed in Fig. 7. The broadening of the activity distribution at 250 and 270°C was caused by a greater amount of noise being present in the measured transients (7). At 240 and 250°C two distinguishable active pools can be clearly seen, as have also been observed by others on Ru and Ni catalysts (20, 34, 35). Thus, it may be assumed that, at 240 and 250°C, two types of carbon (α and β) were able to be hydrogenated to methane. Above 250°C, however, only a single reactive pool was evident, even though the less active species should be more easily detectable at higher temperatures because of the increase in rate. The activities of each pool at the peak maximum (peak values) are shown in Table 6. On increasing the temperature, the activity of each pool shifted towards higher values of k as would be expected. The disappearance of the less active pool above 250°C is accompanied by a sudden jump in the increase of the average site activity k ($= 1/\tau_M$). The fact that k is larger than k_α (peak value) is a consequence of the fact that the average value is impacted by the skewedness of the distribution towards higher values of k and by a bias in averaging towards greater activity. The abundance of the intermediates originating from the α pool remained pretty much constant with temperature. The low value (0.9 μmol/g cat.) for $N_{M\beta}$ at 240°C may be attributed to an inherent detectability problem due to the low activity of the pool at this temperature. An interesting feature of Fig. 7 is the disappearance of the β pool at 260 and 270°C. This may correspond to a favored transformation of β carbon into inactive γ carbon at higher temperatures, or the direct dissociation of CO into γ carbon as mentioned earlier. It is well established that, on a typical methanation catalyst, active carbon is not stable but transforms into an unreactive form at a rate dependent on the temperature if not hydrogenated off (36, 37). This corresponds to our observation of the TOS behavior for two different temperatures (Fig. 2), where a bigger relative decrease in activity with TOS was seen at 270°C.

It is relevant at this point to analyze the evolution of the activity distribution with increasing hydrogen partial pressure (Fig. 8). At the low P_{H_2} of 0.14 bar, only one active pool was observed. As the hydrogen partial pressure was increased the second pool appeared. The broadening of the second pool at 0.35 and 0.72 bar is again due to noise in the raw transients. The shift of the peaks towards higher k (Table 7) is simply a reflection of the increase in surface

TABLE 6

Effect of Temperature on Specific Site Activities from Deconvolution ($P_{H_2} = 0.18$ bar and $P_{CO} = 0.036$ bar, $H_2/CO = 5$)

Temperature (°C)	k_α (s^{-1})	k_β (s^{-1})	k ($=1/\tau_M$) (s^{-1})	$N_{M\alpha}$ (μmol/g cat.)	$N_{M\beta}$ (μmol/g cat.)
240	0.09	0.01	0.14	3.8	0.9
250	0.11	0.02	0.18	2.5	2.5
260	0.18	—	0.31	3.8	—
270	0.20	—	0.36	4.8	—

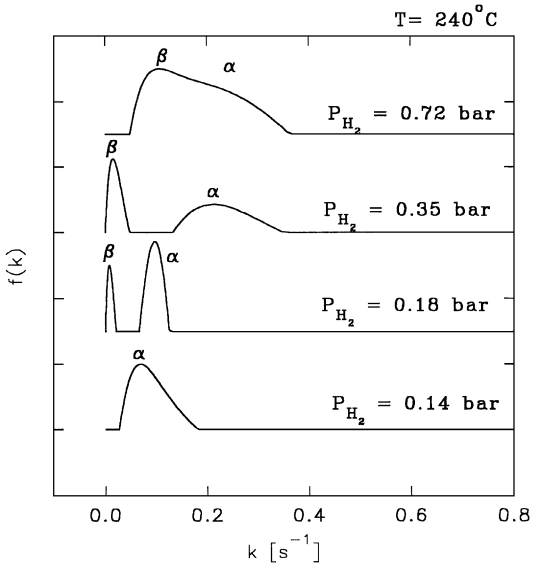

FIG. 8. Activity distributions for different hydrogen partial pressures at 240°C ($P_{CO} = 0.036$ bar).

TABLE 7

Effect of P_{H_2} on Specific Site Activities from Deconvolution ($P_{CO} = 0.036$ bar and $T = 240°C$)

P_{H_2} (bar)	k_α (s^{-1})	k_β (s^{-1})	$k\ (=1/\tau_M)$ (s^{-1})	$N_{M\alpha}$ (μmol/g cat.)	$N_{M\beta}$ (μmol/g cat.)
0.14	0.07	—	0.11	3.4	—
0.18	0.10	0.01	0.14	3.0	0.7
0.35	0.20	0.02	0.20	2.0	2.0
0.72	0.22	0.10	0.30	2.7	2.6

hydrogen concentration, since k contains a dependence on N_H (Eq. [4]). It can also be seen from Table 7 that the increase in hydrogen partial pressure had mainly an impact on the concentration of the less active intermediates concentration ($N_{M\beta}$), $N_{M\alpha}$ remaining essentially constant. As mentioned earlier in the discussion, an increase in surface hydrogen concentration might be expected to weaken the deactivation process. This seems to be the case as evidenced by the appearance of the less active β pool in the activity distribution as hydrogen partial pressure was increased (Fig. 8). The TOS study for two different hydrogen partial pressures (see Fig. 5) also confirms that deactivation was more significant at lower hydrogen partial pressures.

The observations derived from the analysis of the activity distributions can be summarized using Fig. 6: an increase in temperature is presumed to favor step [3] over step [2], corresponding to the disappearance of the β pool in Fig. 7 at higher temperatures. On the other hand, an increase in hydrogen partial pressure appears to favor step [2] over step [3], corresponding to the appearance of the β pool in Fig. 8 at higher hydrogen partial pressures.

CONCLUSIONS

In an isotopic transient kinetic study of methanation on Ru/SiO_2 it was possible to estimate from SSITKA parameters relative surface hydrogen concentrations at constant temperature under reaction conditions. As expected, the relative coverage of hydrogen increased consistently with increasing H_2 partial pressure.

Since a higher hydrogen coverage increases the likelihood for hydrogenation of the surface carbon, this is suggested to have caused the observed increase in the surface coverage of methane intermediates, N_M, with increasing H_2 partial pressure. N_M was in fact a complicated function of H_2 partial pressure, temperature, and deactivation:

(i) At a relatively low H_2 partial pressure (0.18 bar) and H_2/CO ratio ($H_2/CO = 5$), no particular change of N_M with increasing temperature was observed. This is explained by a concomitant partial deactivation of the active sites with increasing temperature at this low hydrogen partial pressure. Two active carbon pools were detected at 240 and 250°C using activity distribution analysis. They were assigned to a more active α and a less active β carbon species which were able to be hydrogenated to methane. Only a single pool of active intermediates (α) was observed above 250°C. This phenomenon is suggested to be caused by a favored transformation of the less active β carbon into inactive γ carbon.

(ii) At a relatively high H_2 partial pressure (0.72 bar) and H_2/CO ratio ($H_2/CO = 20$), N_M increased monotonically with temperature. This was attributed to a more efficient hydrogenation of surface carbon. This hypothesis was also supported by the evolution of the activity distribution with increasing hydrogen partial pressure. At P_{H_2} equal to 0.14 bar only one active pool (α) of active intermediates was observed. As the hydrogen partial pressure was increased above 0.14 bar a less active pool (β) appeared.

ACKNOWLEDGMENT

This study was funded by the National Science Foundation (NSF Grant CTS-9312519) whose support is gratefully acknowledged.

REFERENCES

1. Bennett, C. O., *in* "Catalysis under Transient Conditions," ACS Symposium Series, Vol. 178 (A. T. Bell and L. I., Eds.), Amer. Chem. Soc., Washington, DC, 1982.
2. Happel, J., *Chem. Eng. Sci.* **33**, 1567 (1978).
3. Biloen P., *J. Mol. Catal.* **21**, 17 (1983).
4. Shannon, S. L., and Goodwin, J. G., Jr., *Chem. Rev.* **95**, 677 (1995).
5. Scott, K. F., and Phillips, C. S. G., *J. Chromatogr. Sci.* **21**, 125 (1983).
6. de Pontes, M., Yokomizo, G. H., and Bell, A. T., *J. Catal.* **104**, 147 (1987).
7. Hoost, T. E., and Goodwin, J. G., Jr., *J. Catal.* **134**, 678 (1992).
8. Vannice, M. A., *J. Catal.* **37**, 449 (1975).
9. Vannice, M. A., *J. Catal.* **50**, 228 (1977).
10. Vannice, M. A., *Catal. Rev. Sci. Eng.* **14**, 153 (1976).
11. Haddad, G. J., and Goodwin, J. G., Jr., *J. Catal.* **157**, 25 (1995).
12. Kellner, C. S., and Bell, A. T., *J. Catal.* **70**, 418 (1981).
13. Rodriguez, J. S., and Goodman, D. W., *in* "Studies in Surface Science and Catalysis, volume 64" (L. Gawks, Ed.), Elsevier Science, Amsterdam, 1991.
14. Biloen, P., Helle, J. N., van den Berg, F. G. A., and Sachtler, W. M. H., *J. Catal.* **81**, 450 (1983).
15. Stockwell, D. M., and Bennett, C. O., *J. Catal.* **110**, 354 (1988).
16. Stockwell, D. M., Chung, J. S., and Bennett, C. O., *J. Catal.* **112**, 135 (1988).
17. Winslow, P., and Bell, A. T., *J. Catal.* **158**, 86 (1984).
18. Winslow, P., and Bell, A. T., *J. Catal.* **86**, 158 (1984).
19. Winslow, P., and Bell, A. T., *J. Catal.* **94**, 385 (1985).
20. Hoost, T. E., and Goodwin, J. G., Jr., *J. Catal.* **137**, 22 (1992).
21. McCarty, J. G., and Wise, H., *J. Catal.* **57**, 406 (1979).
22. Chen, B., and Goodwin, J. G., Jr., *J. Catal.* **158**, 511 (1996).
23. Chen, B., and Goodwin, J. G., Jr., *J. Catal.* **148**, 409 (1994).
24. Chen, B., and Goodwin, J. G., Jr., *J. Catal.* **154**, 1 (1995).
25. Tikhonov, A. N., and Arsenin, V. Y., *in* "Solution of Ill-Posed Problems," Wiley, New York, 1977.
26. Biloen, P., Helle, J. N., and Sachtler, W. M. H., *J. Catal.* **58**, 95 (1979).

27. Kellner, C. S., and Bell, A. T., *J. Catal.* **67**, 175 (1981).
28. Ekerdt, J. G., and Bell, A. T., *J. Catal.* **58**, 170 (1979).
29. Anderson, R. B., *in* "The Fischer-Tropsch Synthesis," Academic Press, New York, 1984.
30. Paál, Z., *in* "Hydrogen Effects in Catalysis" (Z. Paál and P. G. Menon, Eds.), Dekker, New York/Basel, 1988.
31. Shum, V. K., Butt, J. B., and Sachtler, W. M. H., *J. Catal.* **99**, 126 (1986).
32. Soong, Y., Krishna, K., and Biloen, P., *J. Catal.* **97**, 330 (1986).
33. Boudart, M., and Djéga-Mariadassou *in* "Kinetics of Heterogeneous Catalytic Reactions," Princeton Univ. Press, Princeton, NJ, 1984.
34. de Pontes, M., Yokomizo, G. H., and Bell, A. T., *J. Catal.* **24**, 147 (1987).
35. Soong, Y., Krishna, K., and Biloen, P., *J. Catal.* **97**, 330 (1986).
36. Wentreck, P. R., Wood, B. J., and Wise, H., *J. Catal.* **43**, 463 (1974).
37. Wise, H., McCarty, J., and Oudar, J., *in* "Deactivation and Poisoning of Catalysts" (J. Oudar and H. Wise, Eds.), Dekker, New York/Basel, 1985.